Clique Identification and Propagation for Multimodal Brain Tumor Image Segmentation

Sidong Liu[1], Yang Song[1], Fan Zhang[1], Dagan Feng[1], Michael Fulham[2,3], Weidong Cai[1]

[1] School of Information Technologies, University of Sydney, Australia
[2] Sydney Medical School, University of Sydney, Australia
[3] Department of PET and Nuclear Medicine, Royal Prince Alfred Hospital, Australia

Abstract. Brain tumors vary considerably in size, morphology, and location across patients, thus pose great challenge in automated brain tumor segmentation methods. Inspired by the concept of clique in graph theory, we present a clique-based method for multimodal brain tumor segmentation that considers a brain tumor image as a graph and automatically segment it into different sub-structures based on the clique homogeneity. Our proposed method has three steps, neighborhood construction, clique identification, and clique propagation. We constructed the neighborhood of each pixel based on its similarities to the surrounding pixels, and then extracted all cliques with a certain size k to evaluate the correlations among different pixels. The connections among all cliques were represented as a transition matrix, and a clique propagation method was developed to group the cliques into different regions. This method is also designed to accommodate multimodal features, as multimodal neuroimaging data is widely used in mapping the tumor-induced changes in the brain. To evaluate this method, we conduct the segmentation experiments on the publicly available Multimodal Brain Tumor Image Segmentation Benchmark (BRATS) dataset. The qualitative and quantitative results demonstrate that our proposed clique-based method achieved better performance compared to the conventional pixel-based methods.

1 Introduction

Gliomas are the most common primary tumors in adults. The median survival for patients with high-grade gliomas is < 2 years and these gliomas account for a disproportionate loss of potential years of life. A patient with a high-grade glioma loses, on average, 12 years of potential life, which is one of the highest for any type of cancer. There is also a high economic cost to families and the community [1, 5]. Neuroimaging is a fundamental component of routine clinical care and research. The routine radiological assessment of magnetic resonance (MR) studies in patients with gliomas includes the delineation of the enhancing rim, regions of cystic / necrotic change, the degree of tumor infiltration and surrounding edema. These routine assessments can have large inter-rater variation, which can relate

to the reader's experience, and could be enhanced by accurate and reproducible measurements of the relevant tumor sub-components such as edema, tumor edge etc. Such indices offer the opportunity to improve image interpretation and assist treatment planning. Delineation of glioma sub-components, however, relies heavily on segmentation techniques. The aim of brain tumor segmentation is to extract the pathologic regions from healthy tissues. Manual segmentation is a slow process and so automated approaches have been explored over the past decade [2–4].

A main challenge for automated methods is that gliomas vary considerably in size, morphology, and location across patients. Intensity gradient between normal and abnormal tissues is the key factor for identifying the glioma. All brain tumor segmentation algorithms assume that if a pixel is similar to its immediate neighbors, then these pixels should be grouped together to represent the same structure. Current brain tumor segmentation algorithms can be categorized as *generative* or *discriminative* models [5]. Generative approaches encode the prior knowledge learned from existing data, such as tumor-specific appearance, or the spatial distribution of different tissues, and then infer the most likely segmentation of the tumor for a given set of brain images based on the tissue spatial distribution patterns [6, 7]. Generative methods need image registration to model the tissue spatial distributions, and it is difficult to transform the semantic descriptions of tumor appearances into appropriate probabilistic models. Discriminative methods avoid modeling these patterns. Instead they use local features, mostly pixel-wise features, e.g., intensity differences or intensity probability distribution of pixels within a patch to infer the segmentation of tumor structures, and classify these pixels / patches as a lesion or non-lesional area using classification algorithms such as support vector machines (SVM), or random forests [8–10]. Discriminative models typically require large amounts of training data to ensure accurate classification performance. This approach is now being used widely as brain tumor imaging data become increasingly available.

The local features in discriminative models are usually extracted from the neighborhoods of pixels [11]. To construct the neighborhood, a straightforward way is to use the standard 4- and 8-pixel neighborhoods [12]. This approach, although widely used, restricts the adaptability to neighborhood variations. For example, a pre-defined neighborhood may contain both a tumor and a non-tumor structure. There are also other algorithms that model the local relationship based on spatial interaction between nearby pixels [13], or a wider spatial context of the pixels [14]. While they can successfully model local information, these methods are usually computationally inefficient. Hence, we present an automated method to extract the local relationship among pixels and to segment the brain tumor into different sub-structures in an effort to increase the effectiveness and efficiency of current discriminative methods. This method is inspired by the concept of clique in graph theory, i.e., a subset of nodes (pixels) in which all of them are mutually connected [15]. Thus, the local relationship is defined at the clique-level instead of at the pixel-level. We also propose a clique propagation scheme for image segmentation based on the inter- and intra-clique variations. Our pro-

posed method is designed to accommodate the various sequences that are used in the MR assessment of gliomas - T2-weighted (T2), T2-weighted fluid-attenuated inversion recovery (FLAIR), T1-weighted (T1), T1-weighted contrast-enhanced with intravenous gadolinium (T1c), diffusion and perfusion sequences. We evaluated our method on the publicly available Multimodal Brain Tumor Image Segmentation Benchmark (BRATS) dataset [5]. We present our findings when compared to the conventional methods that use pixel-wise features.

2 Methods

Our proposed method has three steps. Step 1 is feature extraction and neighborhood construction. Local features are extracted for individual pixels, and used to calculate the similarities between neighboring pixels to construct the neighborhood represented by a pixel adjacency matrix. Step 2 is clique identification. A set of k-clique, each containing k connected pixels, are identified based on the pixel adjacency matrix, and a weighted clique transition matrix is further built to show the connectivity between different cliques. Step 3 is clique propagation, which groups the connected cliques into different tumor sub-structures.

Feature Extraction and Neighborhood Construction Features are firstly extracted from the multi-sequence imaging data to describe the pixels numerically and further to construct the pixel adjacency matrix. Without overemphasizing the feature design, we used the first order texture features in this study. Specifically, mean, variance, skewness and kurtosis were computed from the local patches around the pixels in each of the scans. In this study, each subject had undertaken T1, T1c, T2 and FLAIR sequences. Along with the original multimodal intensities, each pixel p is represented as a 20-dimensional feature vector $V(p)$, as in Eq (1):

$$V(p) = V_{v\in\{T1,T1c,T2,FLAIR\}}(I(p), M(p), V(p), S(p), K(p)) \tag{1}$$

where I, M, V, S, K indicate intensity, mean, variance, skewness and kurtosis for the pixel p. A pixel adjacency matrix PM is constructed to represent the neighborhood information, with $pm(p_i, p_j) = 1$ indicating the two pixels are neighbors. Instead of connecting all pixels within the local patch, a thresholding scheme was adopted to eliminate some dissimilar items for the target pixel. Specifically, cosine similarity was applied to calculate the similarity between pixels based on the feature vectors, and the threshold s_{low} was used to regulate the size of neighborhood for a target pixel p_t, as in Eq (2):

$$pm(p_t, p_j) = 1, \text{ if } cos(V(p_t), V(p_j)) > s_{low} \tag{2}$$

where p_j belongs to the local patch defined for p_t. In our experiments, a 5×5 window with the target pixel in the center was selected as the local patch, which was also used for computing the feature vector. The threshold was set at 0.99 since the pixels are highly similar in terms of the extracted feature vectors.

Clique Identification and Connection The aim of brain tumor segmentation is to find the regions where the pixels are highly homogeneous. The thresholding scheme described above helps to eliminate heterogeneous pixels from the surroundings. However, the direct similarity between pixels is not sufficient to measure the homogeneity without considering the neighbors. So for our method we would like to build the relationship between pixels by further utilizing the neighborhood information. Specifically, the clique is used as the underlying unit to define how the pixels are related.

The concept of clique is introduced in graph theory as a subset of vertices such that every two vertices in this subset are connected. In our study, treating the pixel adjacency matrix as a graph, a k-clique C_k is a group of k pixels that are neighbors to each other, as in Eq (3):

$$C_k = \{p(1), p(2), ..., p(k)\}, \forall i, j \in [1, k], s.t., pm(p(i), p(j)) = 1 \tag{3}$$

The pixels in a clique (triangle) are fully connected, sharing common neighbors with each other, thus these pixels are reinforced mutually and regarded as highly coherent. On the other hand, with the local patch approach, only the most related items are incorporated such that the influence of unrelated pixels in the patch is eliminated. While the pixels in the same clique are considered in the same class, the next step was to identify how pixels from different cliques are related. Specifically, we defined that two cliques are connected if they share common pixels. Supposing there are h $(0 < h < k)$ common pixels, the two cliques are h-connected. According to this, the pixels are considered to be related if the located cliques are connected.

Clique Propagation The relationship of all cliques can be represented as a weighted transition matrix TM in which the weight indicates the connectivity according to h, i.e., $tm(C(i), C(j)) = h$. Starting from a certain clique, clique propagation is conducted by traversing the whole transition matrix to find the connected cliques, which represent one of the regions for the segmentation result. The weights in the transition matrix are used to control the coherence of the connected cliques by reserving connection above the threshold h_{low}, i.e.,

$$tm(C(i), C(j)) = 1, \text{ if } h > h_{low} \tag{4}$$

The clique size k and the threshold h_{low} are two major parameters to determine the segmented region's size. Lowering k and h_{low} will relax the coherence, leading to larger segmented regions. In this study, we selected h_{low} as $k - 1$ so that two cliques were highly connected. The influence of k is discussed in Section 3. Finally, the segmentation result is obtained by finding all connected subsets of cliques.

2.1 Performance Evaluation

As previously indicated we used the publicly available BRATS dataset [5] to evaluate the methods. The dataset contained 30 sets of multi-sequence MR scans

from 10 patients with low-grade (astrocytomas or oligoastrocytomas) and 20 with high-grade (anaplastic astrocytomas and glioblastoma multiforme tumors) gliomas. All subjects had T1, T1c, T2 and FLAIR imaging sequence carried out. Each subject's images were rigidly registered to the T1c scan, and resampled to $1mm$ isotropic resolution in a standardized axial orientation. All scans were manually annotated by up to four human expert raters. Five tumor sub-structures (classes) were labeled for each patient - 'edema' (class 1), 'non-enhancing core' (class 2), 'necrotic core' (class 3), 'active core' (class 4) and others (class 0).

In our experiments, each subject's data were processed at the axial slice-level, and the segmentation result was obtained by combining all slices. Each slice was segmented into different regions with the clique propagation algorithm. The size of clique k was selected manually for each subject. Then, the SVM classifier was used to identify the label of each region based on the average pixel feature within each region. The SVM model was trained using LibSVM [16] with linear kernel by *C-SVC* [17] (with the default parameters, i.e., $gamma$ =1/number of features, $coef0 = 0$, and $degree = 3$). In addition, evaluation was performed from intra- and inter-patient perspectives. For the intra-patient evaluation, the SVM classifier was trained on one slice that crosses the center of the tumor such that all classes were included. For the inter-patient evaluation, the leave-one-subject-out cross-validation was performed.

3 Results

For our method the relationship between pixels was established based on cliques. According to the definition of a clique, a larger clique is composed of multiple small cliques, e.g., a 4-clique contains four 3-cliques. Thus, two pixels are definitely in the same region with 3-clique propagation if they are together with 4-clique propagation, but not vice-versa. In other words, the parameter k can be used to control the size of the segmented regions. The segmentation results of the proposed clique propagation algorithm on an example slice before labeling using the SVM classifier, with $k = 3$ and 4 (shown in the second and third row), is shown in Fig. 1. Compared to the expert segmentation (shown in the first row), the 3-clique propagation can recognize the outline of edema, but it also includes some unexpected tissues, such as necrosis (as indicated with the light green circle in (b)) and a non-tumor region (at bottom). Increasing the clique size to 4, i.e., only 4-cliques are extracted to build the transition matrix, the 4-clique propagation can segment the edema, which is a better segmentation result. Thus, a smaller clique size will lead to an excessively smooth segmentation. On the other hand, while the larger clique size would be helpful to discriminate different structural details, it would also result in over-segmentation. In the experiments, based on our visual inspection, most of subjects in BRATS dataset under study were analyzed with k=4; k=5 was used for a few subjects where the tumors were difficult to identify.

The results of our method, compared to the expert segmentation on two slices from a low-grade and a high-grade tumor, are shown in Fig. 2. For the

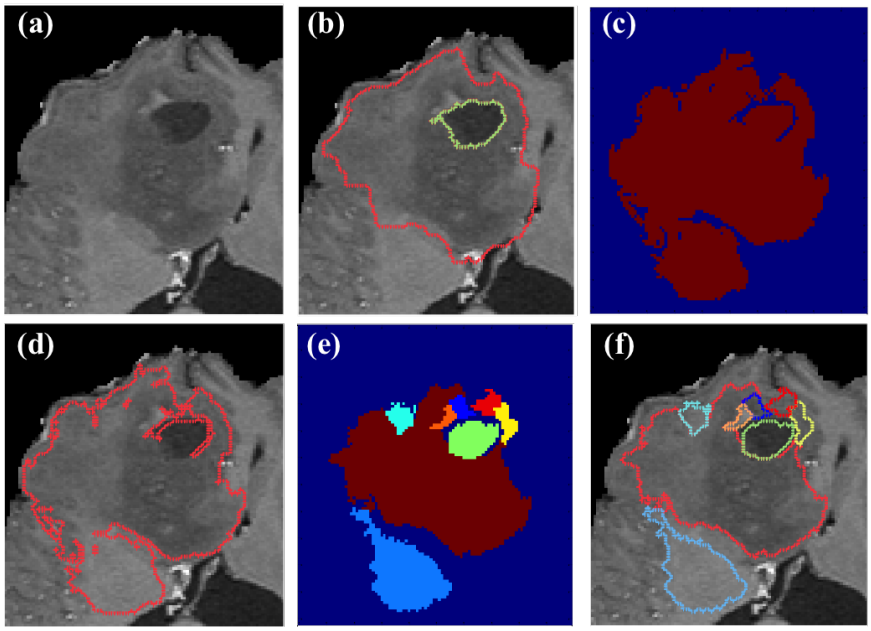

Fig. 1. Comparisons of the clique propagation method with different parameter k. Ground truth: (a) Original cropped MR scan, (b) expert segmentation; 3-clique propagation: (c) region map, (d) segmentation result; 4-clique propagation: (e) region map, (f) segmentation result. The segmented regions are indicated with various colors.

low-grade tumor, the whole tumor outline and necrosis are shown in the first row, and the corresponding segmentation results using our method are given in the second row. For the high-grade case, the whole tumor and tumor core are shown. Visually, it can be seen that our results are reasonably close to the expert labeling.

Quantitative results from the comparison are summarized in Table I. As suggested by Menze et al. [5], the Dice coefficient was computed to describe the performance from three levels: whole tumor (comprising tissue classes 1-4), tumor core (classes 1, 3, and 4) and active tumor (class 4). The second and the third columns show the intra-patient and inter-patient evaluation results. Overall, our method outperformed the SVM approach with a higher Dice coefficient. Since the SVM approach is based on the pixel feature extracted from the local patch, the improvement indicates the advantage of constructing the enforced neighborhood relationship, i.e., the clique. While relatively small improvement was obtained at the whole tumor level, Dice values were better at the tumor and active core levels compared to the SVM approach. This shows that our method is able to identify the small structures that are usually difficult to identify. Nevertheless, the small sized regions are more sensitive to the clique relationship as shown in the intra-patient AC HG segmentation.

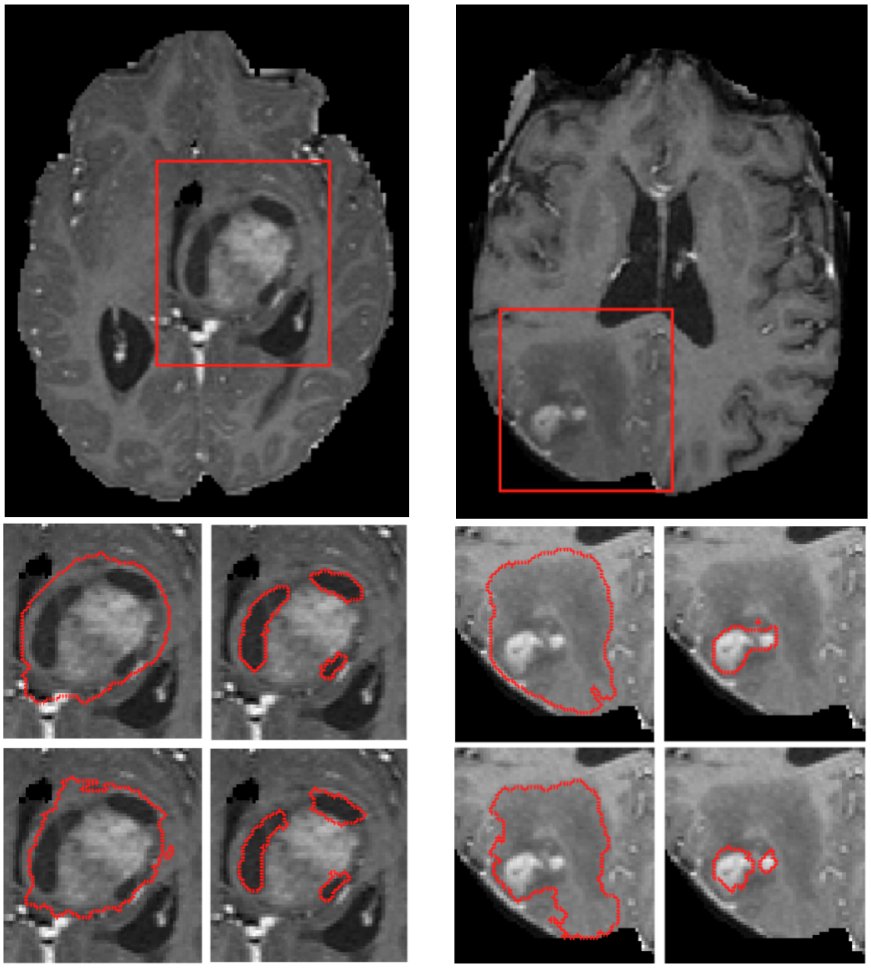

Fig. 2. Transaxial images from a low-grade glioma (left) and a high-grade glioma (right). The expert segmentation results are given in the second row. In the low-grade glioma, contours of the tumor with minimal surrounding edema and cystic elements are shown; in the high-grade glioma, the edema and tumor core contours are displayed. Our segmentation results are shown in the third row.

Table 1. Average DICE coefficient for the 10 patients with low-grade (LG) and 20 with high-grade (HG) gliomas for whole tumor (WT), tumor core (TC) and active core (AC).

	Intra-Patient		Inter-Patient	
	SVM	Proposed	SVM	Proposed
WT LG	0.821	**0.825**	0.710	**0.757**
WT HG	0.678	**0.708**	0.607	**0.619**
TC LG	0.625	**0.705**	0.388	**0.536**
TC HG	0.569	**0.653**	0.358	**0.469**
AC LG	0.622	**0.699**	0.176	**0.512**
AC HG	**0.661**	0.641	0.199	**0.410**

4 Conclusions and Future Works

In this paper, we present a clique-based algorithm for brain tumor segmentation in multi-sequence MR scan data. All cliques were identified based on the neighborhood of each pixel and the relationship between pixels was built from intra- and inter-clique perspectives in terms of the connections among cliques. The clique propagation algorithm was used to finalize the segmentation. We applied it to a publicly available glioma dataset (BRATS). Our approach was superior to the SVM-based approach. Since our method does not specifically depend on any features, we used the simplest features, such as mean and variance in the imaging data. We would expect a better performance when using customized features for different imaging modalities.

In future work we will design novel features to capture the complex characteristics of human gliomas. Currently, the weight for transition matrix, the selection of h_{low}, and clique size k are determined empirically, so we will investigate intelligent methods to select these parameters and then evaluate them.

References

1. E.C. Holland, "Progenitor cells and glioma formation," Current Opinion in Neurology, vol. 14, pp. 683-688, 2001.
2. S. Bauer, R. Wiest, L.-P. Nolte, and M. Reyes, "A survey of MRI-based medical image analysis for brain tumor studies," Physics in Medicine and Biology, vol. 58, no. 13, pp. 97-129, 2013.
3. S. Liu, W. Cai, S. Q. Liu, F. Zhang, M. J. Fulham, D. Feng, S. Pujol, R. Kikinis, "Multimodal neuroimaging computing: a review of the applications in neuropsychiatric disorders," Brain Informatics (BRIN), vol. 2, no. 3, pp. 167-180, 2015.
4. S. Liu, W. Cai, S. Q. Liu, F. Zhang, M. J. Fulham, D. Feng, S. Pujol, R. Kikinis, "Multimodal neuroimaging computing: the workflows, methods, and platforms," Brain Informatics (BRIN), vol. 2, no. 3, pp. 181-195, 2015.
5. B. Menze, A. Jakab, S. Bauer, J. Kalpathy-Cramer, K. Farahani, J. Kirby, et al., "The Multimodal Brain Tumor Image Segmentation Benchmark (BRATS)," IEEE Transactions on Medical Imaging, vol. 34, no. 10, pp. 1993-2024, 2014.

6. J. J. Corso, E. Sharon, S. Dube, S. El-Saden, U. Sinha, and A. Yuille, "Efficient multilevel brain tumor segmentation with integrated bayesian model classification," IEEE Transactions on Medical Imaging, vol. 27, no. 5, pp. 629-640, 2008.
7. K. M. Pohl, J. Fisher, J. J. Levitt, M. E. Shenton, R. Kikinis, W. E. L. Grimson, et al., "A unifying approach to registration, segmentation, and intensity correction," in MICCAI, ed: Springer, vol. 3749, pp. 310-318, 2005.
8. S. Parisot, H. Duffau, S. Chemouny, and N. Paragios, "Graph-based detection, segmentation & characterization of brain tumors," in CVPR, pp. 988-995, 2012.
9. M. Wels, G. Carneiro, A. Aplas, M. Huber, J. Hornegger, and D. Comaniciu, "A discriminative model-constrained graph cuts approach to fully automated pediatric brain tumor segmentation in 3-D MRI," in MICCAI, ed: Springer, vol. 5241, pp. 67-75, 2008.
10. K. M. Pohl, S. Bouix, R. Kikinis, and W. E. L. Grimson, "Anatomical guided segmentation with non-stationary tissue class distributions in an expectation-maximization framework," in IEEE International Symposium on Biomedical Imaging: Nano to Macro, vol.1, pp. 81-84, 2004.
11. D. L. Pham, C. Xu, and J. L. Prince, "Current methods in medical image segmentation 1," Annual review of biomedical engineering, vol. 2, pp. 315-337, 2000.
12. S. Z. Li and S. Singh, Markov random field modeling in image analysis, Springer London, vol. 3, 2009.
13. N. K. Subbanna, D. Precup, D. L. Collins, and T. Arbel, "Hierarchical Probabilistic Gabor and MRF Segmentation of Brain Tumours in MRI Volumes," in MICCAI, ed: Springer, vol. 8149, pp. 751-758, 2013.
14. S. Bauer, L.-P. Nolte, and M. Reyes, "Fully automatic segmentation of brain tumor images using support vector machine classification in combination with hierarchical conditional random field regularization," in MICCAI, ed: Springer, vol.6893, pp. 354-361, 2011.
15. D. B. West, Introduction to graph theory, vol. 2: Prentice hall Upper Saddle River, 2001.
16. C.-C. Chang and C.-J. Lin, "LIBSVM: a library for support vector machines," ACM Transactions on Intelligent Systems and Technology (TIST), vol. 2, pp. 1-27, 2011.
17. B. E. Boser, I. M. Guyon, and V. N. Vapnik, "A training algorithm for optimal margin classifiers," in Proceedings of the fifth annual workshop on Computational learning theory, pp. 144-152, 1992.